The Plant Cell, Vol. 25: 3858–3870, October 2013, www.plantcell.org

Regulation of Auxin Homeostasis and Gradients in *Arabidopsis* Roots through the Formation of the Indole-3-Acetic Acid Catabolite 2-Oxindole-3-Acetic Acid[C][W][OPEN]

Aleš Pěnčík,[a] Biljana Simonovik,[a,1] Sara V. Petersson,[a,2] Eva Henyková,[a,c] Sibu Simon,[d,3] Kathleen Greenham,[e,4] Yi Zhang,[e] Mariusz Kowalczyk,[a,5] Mark Estelle,[e] Eva Zažímalová,[d] Ondřej Novák,[a,c] Göran Sandberg,[b] and Karin Ljung[a,6]

[a] Umeå Plant Science Centre, Department of Forest Genetics and Plant Physiology, Swedish University of Agricultural Sciences, SE-901 83, Umea, Sweden

[b] Umeå Plant Science Centre, Department of Plant Physiology, Umeå University, SE-901 87, Umea, Sweden

[c] Laboratory of Growth Regulators, Faculty of Science, Palacký University and Institute of Experimental Botany, Academy of Sciences of the Czech Republic, 783 71 Olomouc, Czech Republic

[d] Institute of Experimental Botany, Academy of Sciences of the Czech Republic, 16502 Prague 6, Czech Republic

[e] Section of Cell and Developmental Biology, University of California at San Diego, La Jolla, California 92093

ORCID ID: 0000-0003-2901-189X (K.L.).

The native auxin, indole-3-acetic acid (IAA), is a major regulator of plant growth and development. Its nonuniform distribution between cells and tissues underlies the spatiotemporal coordination of many developmental events and responses to environmental stimuli. The regulation of auxin gradients and the formation of auxin maxima/minima most likely involve the regulation of both metabolic and transport processes. In this article, we have demonstrated that 2-oxindole-3-acetic acid (oxIAA) is a major primary IAA catabolite formed in *Arabidopsis thaliana* root tissues. OxIAA had little biological activity and was formed rapidly and irreversibly in response to increases in auxin levels. We further showed that there is cell type–specific regulation of oxIAA levels in the *Arabidopsis* root apex. We propose that oxIAA is an important element in the regulation of output from auxin gradients and, therefore, in the regulation of auxin homeostasis and response mechanisms.

INTRODUCTION

Auxin is an important signaling molecule in plants, with the level and type of response that it triggers dependent on both its concentration and downstream signaling events (reviewed in Sauer et al., 2013). At the site of action, auxin signaling is initiated through binding of the hormone to the TRANSPORT INHIBITOR RESPONSE1/AUXIN SIGNALING F-BOX PROTEIN (TIR1/AFB) and AUXIN/INDOLE ACETIC ACID (Aux/IAA) protein coreceptors and the consequent targeting of the Aux/IAA proteins for degradation (Dharmasiri et al., 2005; Kepinski and Leyser, 2005; Calderón-Villalobos et al., 2012). The indole-3-acetic acid (IAA) molecule is believed to act as "molecular glue" between the TIR1/AFB and Aux/IAA proteins (Calderon-Villalobos et al., 2010). Small changes in the structure of the IAA molecule, therefore, could have a strong impact on the binding affinity of these proteins to IAA and attenuate the degradation of Aux/IAAs and the IAA response. It has been suggested that auxin acts as a morphogen, altering the developmental fate of cells in a concentration-specific manner (Bhalerao and Bennett, 2003). Whether or not auxin fulfills the strict definition of a morphogen or acts as a morphogenetic trigger (Benková et al., 2009), it is clear that setting up auxin concentration gradients requires a strict regulation of many different cellular processes. The concentration of auxin within a plant cell is regulated both by the rate of its metabolism (i.e., biosynthesis, conjugation/deconjugation, and degradation) and the capacity and rate of transport (in and out of cells and between cellular compartments).

There are at least four classes of IAA transporters in plants, the PIN-FORMED (PIN), PIN-LIKES (PILS), AUXIN RESISTANT1/LIKE AUXIN RESISTANT (AUX1/LAX), and ATP BINDING CASSETTE SUBFAMILY B TRANSPORTER (ABCB) proteins (reviewed in Zažímalová et al., 2010). The AUX1/LAX and some PIN proteins are auxin influx and efflux carriers, respectively, and the polar localization of these transporters in specific cells is critical for differential auxin distribution during plant development. PIN5, PIN6, and PIN8 and the newly discovered PILS proteins are

[1] Current address: 160 Erskine Avenue Apt, Toronto M4P 123, Canada.
[2] Current address: BioVis, Department for Immunlogy, Genetics, and Pathology, Uppsala University, Rudbecklaboratoriet, SE-751 85, Uppsala, Sweden.
[3] Current address: Institute of Science and Technology, 3400 Klosterneuburg, Austria.
[4] Current address: Department of Biological Sciences, Dartmouth College, Hanover, New Hampshire 03755.
[5] Current address: Department of Biochemistry and Crop Quality, Institute of Soil Science and Plant Cultivation, State Research Institute, 24-100 Pulawy, Poland.
[6] Address correspondence to karin.ljung@slu.se.
The author responsible for distribution of materials integral to the findings presented in this article in accordance with the policy described in the Instructions for Authors (www.plantcell.org) is: Karin Ljung (karin.ljung@slu.se).
[C] Some figures in this article are displayed in color online but in black and white in the print edition.
[W] Online version contains Web-only data.
[OPEN] Articles can be viewed online without a subscription.
www.plantcell.org/cgi/doi/10.1105/tpc.113.114421

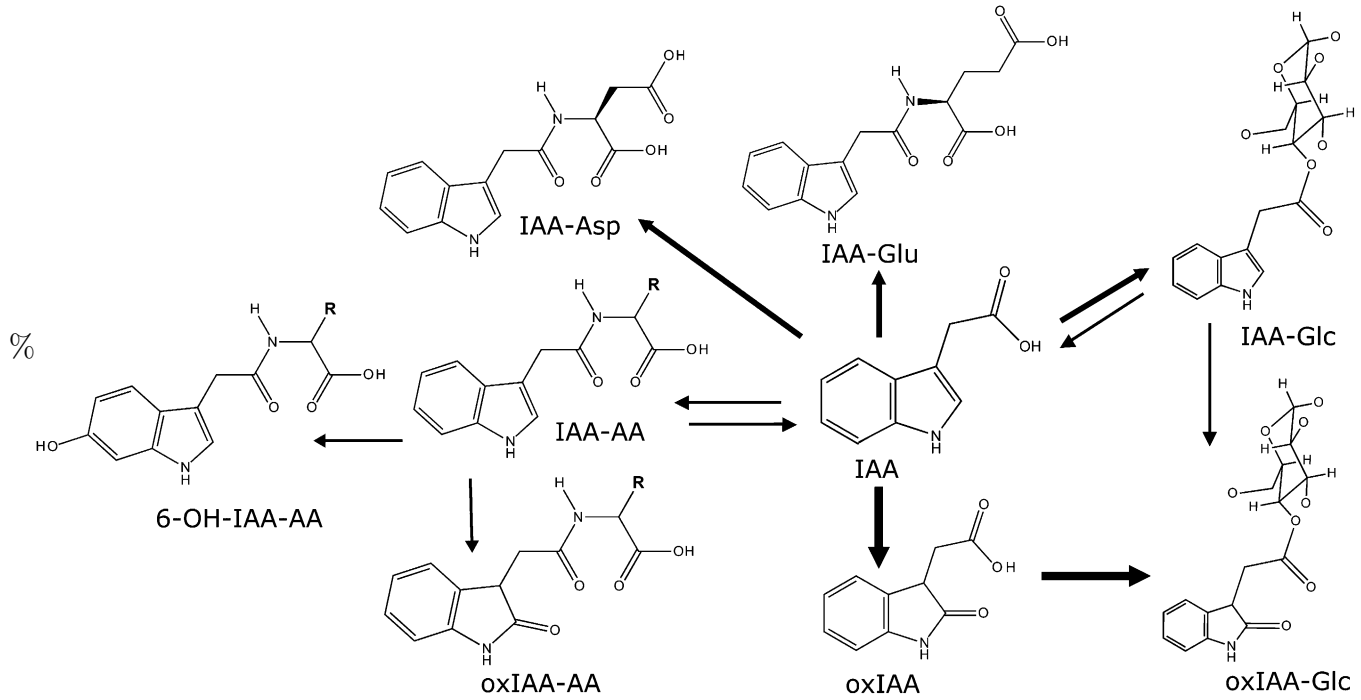

Figure 1. Major Routes for IAA Degradation in *Arabidopsis*.

Oxidation of IAA to oxIAA, and subsequent conjugation with Glc to form oxIAA-Glc, is a major route for IAA catabolism in *Arabidopsis*, based on feeding experiments with labeled precursors and mass spectrometry-based quantification of IAA metabolites (Östin et al., 1998; Kowalczyk and Sandberg, 2001; Kai et al., 2007; Kubeš et al., 2012; Peer et al., 2013). IAA can also be conjugated to either Glc or amino acids (AA), and these compounds can be further metabolized to oxIAA-Glc, 6-OH-IAA-AA, and oxIAA-AA. Some of these conjugates may act as reversible storage forms of IAA that can later be hydrolyzed to produce free IAA. The most abundant AA conjugates in *Arabidopsis* seedlings are normally IAA-Asp and IAA-Glu (Östin et al., 1998; Tam et al., 2000; Kowalczyk and Sandberg, 2001; Kai et al., 2007; Novák et al., 2012).

believed to be involved in the regulation of intracellular auxin homeostasis (Mravec et al., 2009; Barbez et al., 2012; Dal Bosco et al., 2012; Ding et al., 2012). The ATP-dependent ABCB transporters do not show the same polarized localization in the cells, but data indicate that they are likely to be important both for long-distance auxin transport and for local auxin gradient and auxin maxima/minima formation (Zažímalová et al., 2010). Long-distance transport from the shoot supplies the root apex with auxin (reviewed in Robert and Friml, 2009), but auxin is also produced in situ within the root apex, with maximum synthesis centered on the quiescent center and stem cells (Ljung et al., 2005; Stepanova et al., 2008; Petersson et al., 2009). The polar localization of auxin efflux carriers in the root tip suggests that auxin is transported via the stele to the root apex, where it is rerouted through the columella and lateral root cap to the epidermis, affecting processes such as root elongation and gravitropic responses (reviewed in Robert and Friml, 2009).

The most comprehensively studied IAA biosynthetic pathways rely on Trp as a precursor (reviewed in Normanly, 2010; Korasick et al., 2013; Ljung, 2013). Recent data have shown the importance of Trp-dependent IAA biosynthesis in numerous plant processes. Genes and pathways involved in Trp-dependent IAA biosynthesis have been identified in *Arabidopsis thaliana* (Zhao et al., 2001; Stepanova et al., 2008, 2011; Tao et al., 2008; Sugawara et al., 2009; Yamada et al., 2009; Mashiguchi et al., 2011; Won et al., 2011) and other plant species (Yamamoto et al., 2007; Gallavotti et al., 2008; Quittenden et al., 2009). Importantly, mechanisms to reduce the levels of free auxin, such as conjugation and degradation, are also believed to be essential for maintaining appropriate cellular auxin levels. However, our understanding of these processes and their relative importance remains rudimentary. It is known that auxin can be conjugated to amino acids and sugars to either storage forms or to irreversible degradation products, and several genes involved in IAA conjugation and deconjugation have been identified (reviewed in Ludwig-Müller, 2011; Korasick et al., 2013). Data from our laboratory and others have demonstrated that oxidation of IAA to 2-oxindole-3-acetic acid (oxIAA) is another important pathway for IAA degradation in plant species such as *Arabidopsis* (Östin et al., 1998; Kowalczyk and Sandberg 2001; Kai et al., 2007; Novák et al., 2012; Peer et al., 2013), maize (*Zea mays*; Reinecke and Bandurski, 1983), and *Pinus sylvestris* (Ernstsen et al., 1987). These findings have mainly been based on the use of radioactive and labeled precursor feeding and/or mass spectrometry identification and quantification of the main IAA degradation products. To our knowledge, no genes and/or enzymes have so far been identified in IAA catabolic/oxidation

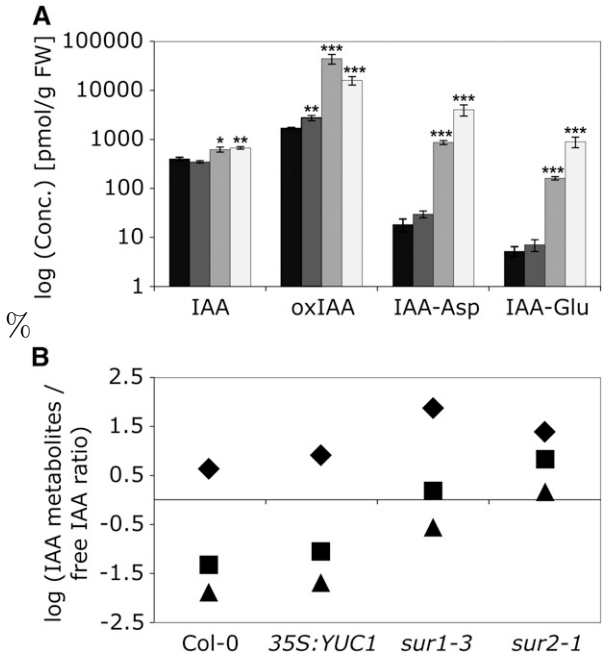

Figure 2. Concentrations of IAA Metabolites in IAA-Overproducing *Arabidopsis* Mutant Lines.

Free IAA, the catabolite oxIAA, and the conjugates IAA-Asp and IAA-Glu were quantified in root tissues from 10-DAG wild-type *Arabidopsis* Col-0 and IAA-overproducing lines (*35S*:*YUC1*, *sur1-3*, and *sur2-1*).

(A) Logarithmic concentration (pmol g^{-1} fresh weight) of IAA, oxIAA, IAA-Asp, and IAA-Glu in *Arabidopsis* Col-0 (black bars) and the mutant lines *35S*:*YUC1*, *sur1-3*, and *sur2*-1 (dark to light gray bars, respectively). Error bars indicate SD (n = 3). Asterisks indicate statistically significant differences in the mutant lines (*35S*:*YUC1*, *sur1-3*, and *sur2-1*) versus the wild type (Col-0) in an ANOVA analysis (one, two, and three asterisks correspond to $0.05 > P > 0.01$, $0.01 > P > 0.001$, and $P < 0.001$, respectively). FW, Fresh weight.

(B) Logarithmic ratio between the concentration of IAA metabolites and free IAA (diamonds, oxIAA/IAA; squares, IAA-Asp/IAA; triangles, IAA-Glu/IAA) in the different *Arabidopsis* lines.

pathways in plants, making it difficult to study the specific regulation and function of IAA catabolism in planta.

This article offers important insights into the function of IAA catabolism and shows that oxIAA is a major primary IAA catabolite formed in *Arabidopsis* root tissues. We have shown that irreversible degradation of IAA to oxIAA, a molecule with very low auxin activity, is an important mechanism for removing active auxin from the root tip. An oxIAA gradient with its maxima following the IAA gradient, consistent with oxIAA formation as an end point for IAA metabolism in the root apex, was also demonstrated. We also observed that there are cell types in this region with a higher capacity to inactivate IAA than others and that oxIAA is inactive in cell elongation assays, in auxin signaling, and in auxin transport across cell membranes. Taken together, these data indicate that oxidation of IAA to oxIAA is an important regulator of IAA homeostasis, capable of modulating developmentally important auxin gradients and auxin maxima/minima in plants.

RESULTS

IAA-Overproducing *Arabidopsis* Mutant Lines Form Large Amounts of IAA Degradation Products

Based on isotope feeding experiments and mass spectrometry identification and quantification of IAA metabolites, we have previously identified the major primary IAA catabolites and conjugates in *Arabidopsis* as oxIAA, IAA-Glu, and IAA-Asp (Östin et al., 1998; Kowalczyk and Sandberg, 2001; Figure 1). These compounds can then be further metabolized to oxIAA-Glc, oxIAA-Asp, and hydroxy(OH)-IAA-Asp (Östin et al., 1998; Kai et al., 2007). Additional IAA metabolites have been identified in *Arabidopsis*, such as IAA-Glc, IAA-Val, IAA-Phe, 6-OH-IAA-Val, and 6-OH-IAA-Phe (Kai et al., 2007), IAA-Trp (Staswick 2009), and IAA-Ala and IAA-Leu (Kowalczyk and Sandberg, 2001; Rampey et al., 2004). These and other studies (Tam et al., 2000; Kubeš et al., 2012; Novák et al., 2012; Peer et al., 2013) clearly show that oxIAA is a major IAA degradation product in *Arabidopsis* tissues and that IAA amino acid conjugates are normally present in much lower quantities.

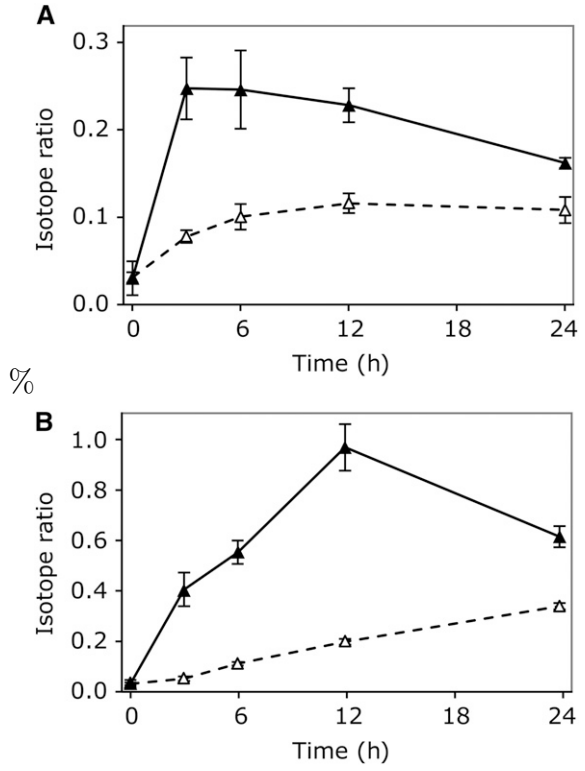

Figure 3. In Vivo Labeling of IAA and OxIAA.

The incorporation of [$^{15}N_1$]anthranilate **(A)** and [$^{15}N_1$]indole **(B)** into IAA (closed triangles) and oxIAA (open triangles) was monitored after feeding 7-DAG wild-type *Arabidopsis* Col-0 seedlings with liquid medium containing 10 μM of the labeled precursor for 3, 6, 12, and 24 h. Enrichment of the IAA and oxIAA pools is expressed as the isotope ratio, the ratio of labeled to unlabeled compound, after correction for natural isotope abundances. Error bars indicate SD (n = 3).

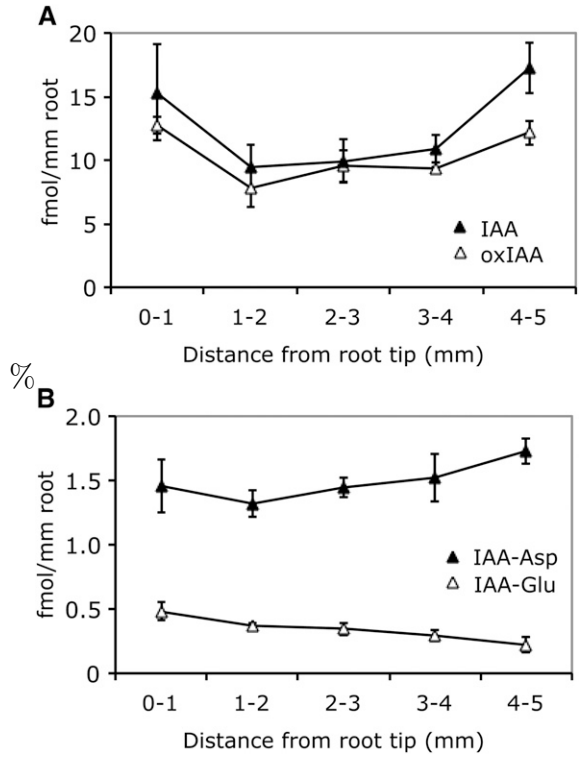

Figure 4. Concentrations of IAA Metabolites in the *Arabidopsis* Root Apex.

Free IAA (**[A]**; closed triangles), the catabolite oxIAA (**[A]**; open triangles), and the IAA conjugates IAA-Asp (**[B]**; closed triangles) and IAA-Glu (**[B]**; open triangles) were quantified in 1-mm sections of the primary root apex from 6-DAG wild-type *Arabidopsis* Col-0 seedlings. Error bars indicate SD (n = 3).

In order to ascertain the major contributors to the conjugation and degradation of IAA, we analyzed the concentration of the hormone and the major catabolites and conjugates in root tissue from the three IAA-overproducing mutants *YUCCA1* (*35S*:*YUC1*; Zhao et al., 2001), *superoot1-3* (*sur1-3*; Boerjan et al., 1995; Mikkelsen et al., 2004), and *sur2-1* (Barlier et al., 2000) at 10 d after germination (DAG; Figure 2). The *YUC1* gene is believed to be directly involved in Trp-dependent IAA biosynthesis, while the *sur1-3* and *sur2-1* mutations block indole glucosinolate biosynthesis, thereby redirecting metabolism into IAA biosynthesis, resulting in IAA overproduction (reviewed in Ljung, 2013). Both *sur1-3* and *sur2-1* show increased IAA levels in root tissues from 10-DAG seedlings compared with the wild-type ecotype Columbia (Col-0), while the difference between the wild type and *35S*:*YUC1* is less pronounced (Figure 2A). *sur1-3* and *sur2-1* seedlings also show a strong accumulation of oxIAA in the root compared with the wild type (Figure 2A). The concentrations of the IAA conjugates IAA-Asp and IAA-Glu are low in the roots of *Arabidopsis* wild-type seedlings. By comparison, the compounds are elevated in *sur1-3* and *sur2-1* seedlings, but their concentrations remain much lower than for oxIAA (Figure 2A). We also compared the ratios between the concentrations of these three IAA metabolites and IAA. For wild-type Col-0 and the mutant lines *35S*:*YUC1*, *sur1-3*, and *sur2-1*, the ratio between oxIAA and IAA was much higher than the ratios IAA-Asp:IAA and IAA-Glu:IAA (Figure 2B).

The IAA and OxIAA Pools Are Rapidly Labeled after Feeding with Labeled IAA Precursors

We then performed a feeding experiment to study the comparative synthesis rates of IAA and oxIAA, using heavily labeled anthranilate and indole as IAA precursors. Seven-day-old *Arabidopsis* seedlings were incubated with liquid medium containing either 10 μM [$^{15}N_1$]anthranilate or 10 μM [$^{15}N_1$]indole for 3 to 24 h. The incorporation of the precursors into IAA and oxIAA was measured using liquid chromatography–tandem mass spectrometry (LC-MS/MS). De novo synthesis of IAA was rapid, and a strong enrichment of the IAA pool was already observed after 3 h (Figure 3). Labeled IAA peaked at 3 h after feeding with [$^{15}N_1$]anthranilate (Figure 3A) and at 12 h after feeding with [$^{15}N_1$]indole (Figure 3B). Labeling of the oxIAA pool was slower than for IAA, even though an increase in the pool of labeled oxIAA could be observed already after 3 to 6 h (Figures 3A and 3B). This showed that labeled IAA precursors are rapidly incorporated into IAA and the catabolic pathway product oxIAA.

OxIAA Is a Major IAA Degradation Product in the *Arabidopsis* Root Apex

In order to better understand the importance of IAA degradation for the regulation of IAA homeostasis and the formation of the IAA gradient in the root apex, we analyzed IAA, the major IAA catabolite oxIAA, and the IAA conjugates IAA-Glu and IAA-Asp in 1-mm sections of the primary root tip from 6-DAG wild-type *Arabidopsis* (Col-0) seedlings. The concentration gradient of oxIAA closely matched that of IAA, with almost constant oxIAA:IAA concentration ratios in the different root sections (Figure 4A). In contrast, the concentrations of the conjugates IAA-Asp and IAA-Glu were 10- and 30-fold lower than that of IAA in the root tip, respectively, and the concentration was low and constant throughout the root apex (Figure 4B).

Previous studies have shown that when 14-DAG *Arabidopsis* seedling roots are treated with radiolabeled IAA, the primary degradation products are oxIAA, oxIAA-Glc, IAA-Asp, and IAA-Glu (Östin et al., 1998). To study the kinetics of the metabolic pathways responsible for IAA degradation in the root, we performed feeding experiments in which radioactive labeled IAA was applied to whole *Arabidopsis* seedlings and to intact roots, and the degradation of IAA was measured by radioactivity detection or scintillation counting after separation of the metabolites by HPLC. Feeding exogenous IAA to whole seedlings for 8 h resulted in the formation of the metabolites oxIAA-Glc, oxIAA, IAA-Asp, IAA-Glu, and IAA-Ala (Figure 5A, peaks 1–5, respectively), in accordance with previous observations (Östin et al., 1998; Kowalczyk and Sandberg 2001). When applied to the cut surface of intact roots, exogenous IAA was quickly transported down through the root system and metabolized, mainly to oxIAA and oxIAA-Glc (Figure 5B). The predominant metabolite in protoplasts isolated from roots fed with radioactive labeled IAA was oxIAA, indicating that oxidation through this

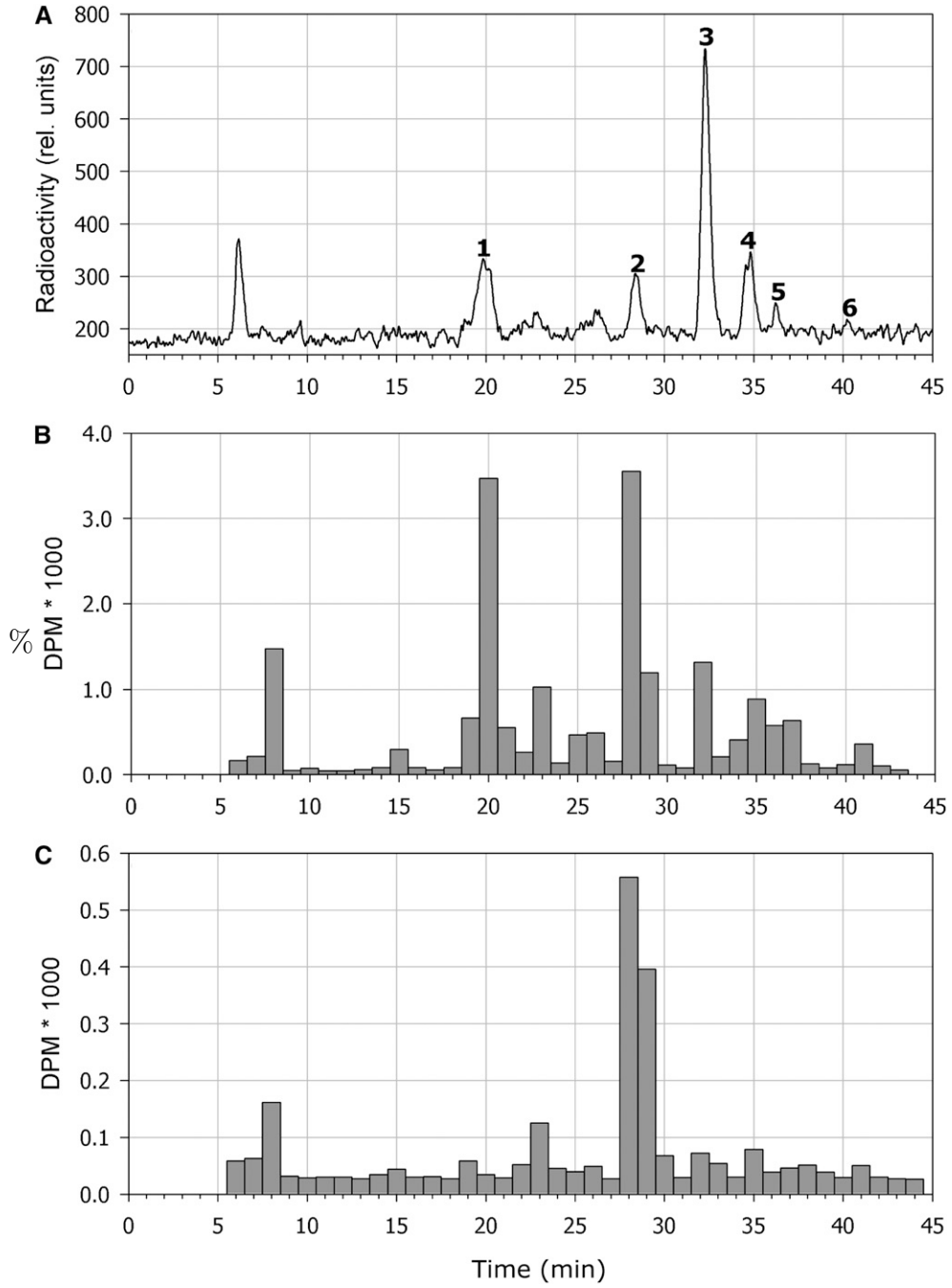

Figure 5. Profiling of IAA Metabolites after Feeding with Radiolabeled IAA.

Radioactivity profiles are shown for IAA metabolites in extracts from whole seedlings **(A)**, intact root tips **(B)**, and isolated root tip protoplasts **(C)** after feeding 7-DAG *Arabidopsis* wild-type Col-0 seedlings with [1′-^{14}C]IAA. IAA and its metabolites were separated using HPLC, and the radioactivity in dpm was monitored using scintillation counting. After feeding of whole seedlings **(A)**, almost all of the [1′-^{14}C]IAA that was taken up was rapidly degraded to radioactive oxIAA-Glc (peak 1), oxIAA (peak 2), IAA-Asp (peak 3), IAA-Glu (peak 4), and IAA-Ala (peak 5), and very little radioactive IAA (peak 6) was remaining in the extract. Radioactive IAA applied to excised roots was quickly transported down to the root apex and metabolized into mainly oxIAA and oxIAA-Glc **(B)**. In isolated protoplasts, oxIAA was the major metabolite observed **(C)**.

compound is the primary mechanism of IAA deactivation (Figure 5C). We also performed feeding experiments with unlabeled IAA. Intact 8-DAG seedlings were incubated with and without 10 μM IAA for 5.5 h, and the increase in the concentration of oxIAA in the root apex was analyzed using LC-MS/MS. The concentration of oxIAA more than doubled after IAA treatment (Figure 6). Taken together, our data suggest that the formation of IAA conjugates probably plays a limited role in IAA homeostasis within the *Arabidopsis* root apex and that oxidation of IAA to oxIAA is the most important mechanism for IAA deactivation in this tissue.

Cell-Specific Analysis of IAA and OxIAA in the *Arabidopsis* Root Apex

We then analyzed the levels of IAA and oxIAA in *Arabidopsis* lines expressing green fluorescent protein (GFP) in different cell types of the root to determine if there was a difference in IAA catabolism between cell types. The GFP-expressing cell lines J2812:GFP, *pWOODEN LEG*:*GFP* (*pWOL*:*GFP*), *pSCARECROW*:*GFP* (*pSCR*:*GFP*), and M0028:GFP were chosen so that all cell types in the root apex were covered (Figure 7A). We have previously shown that the cell types represented by these lines synthesize IAA at a high rate compared with the remainder of the root (Petersson et al., 2009). Seedlings were grown for 8 d on vertical plates in long-day (LD) conditions, and the roots were harvested for protoplasting and fluorescence-activated cell sorting (FACS) analysis. During cell sorting, the protoplasts were sorted into GFP-expressing cells (GFP+) and nonfluorescent cells (GFP−), which enabled the use of specific reference populations for each biological replicate of GFP+ cells.

The concentration of IAA and oxIAA was measured in both the GFP+ and GFP− samples using LC-MS/MS, and the ratio in metabolite concentration between the GFP+ and GFP− cell populations was calculated for oxIAA (Figure 7B) and IAA (Figure 7C), respectively. In the J2812:GFP line, GFP is expressed in the

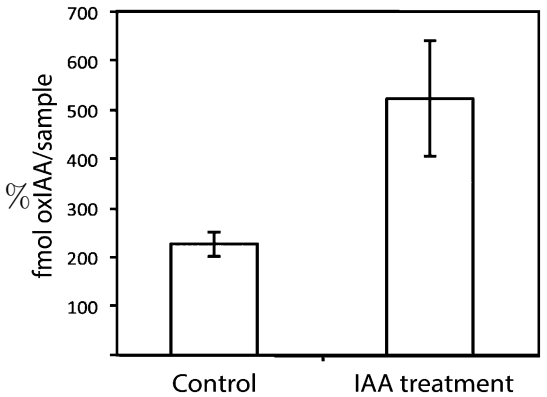

Figure 6. Conversion of Exogenous IAA to OxIAA in the *Arabidopsis* Root Apex.

Wild-type *Arabidopsis* Col-0 seedlings were treated at 8 DAG with and without 10 μM IAA for 5.5 h, and the concentration of oxIAA in the root apex (pooled 5-mm sections of the root tip) was analyzed by LC-MS/MS. Error bars represent SD (n = 5).

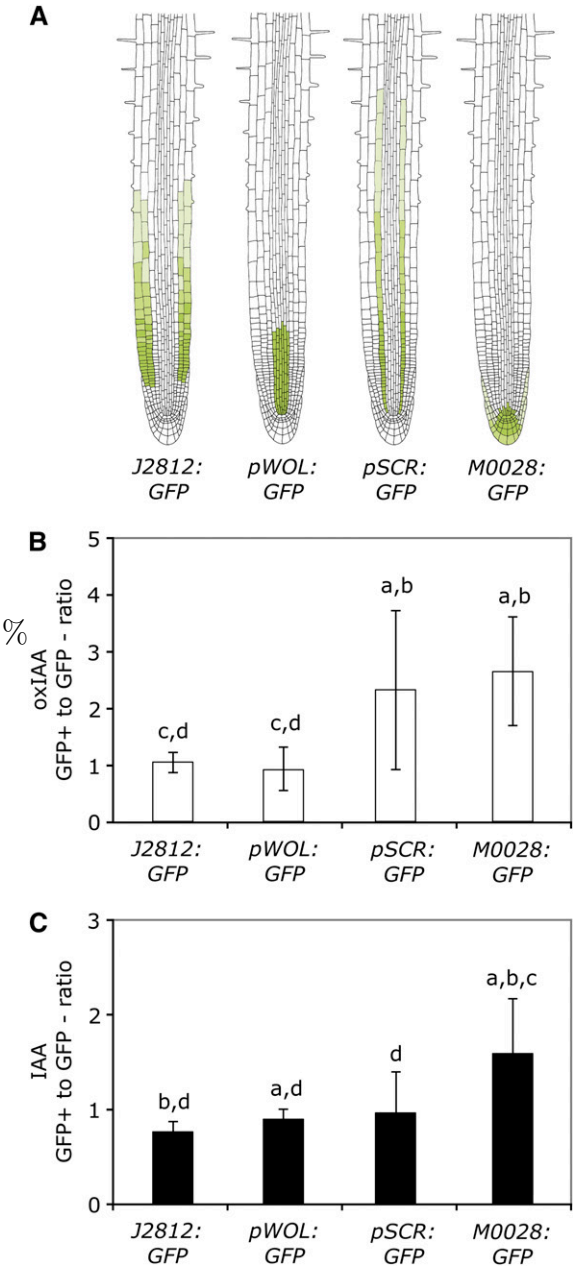

Figure 7. OxIAA and IAA Levels in Four Different Cell Types Isolated from the *Arabidopsis* Root.

Roots from 8-DAG *Arabidopsis* seedlings expressing GFP in specific cell types were protoplasted and sorted using FACS, and the concentrations of IAA and oxIAA were quantified in the collected GFP+ and GFP− cell populations using LC-MS/MS.

(A) GFP expression patterns of the *Arabidopsis* lines J2812:GFP, *pWOL*:*GFP*, *pSCR*:*GFP*, and M0028:GFP.

(B) and **(C)** For each of the four GFP lines, the ratio between the oxIAA **(B)** and IAA **(C)** concentrations in the GFP+ and GFP− cell populations was calculated. Error bars indicate SD (n = 7–11). Letters above the bars are as follows: a, significantly different from J2812:GFP; b, significantly different from *pWOL*:*GFP*; c, significantly different from *pSCR*:*GFP*; d, significantly different from M0028:GFP (Student's t test, $P < 0.05$).

[See online article for color version of this figure.]

epidermis and cortex, while in the *pWOL*:*GFP* line, GFP is expressed in the stele (Figure 7A). Both these lines show a relatively low ratio between GFP+ and GFP− cells for oxIAA formation compared with the *pSCR*:*GFP* and M0028:GFP lines (Figure 7B). In the M0028:GFP line, GFP is expressed in the root cap, the columella, the columella initials, and the quiescent center, and in the *pSCR*:*GFP* line, GFP is expressed in the endodermis. Our data suggest that these cell types have a higher rate of IAA catabolism (Figure 7B). They also show a greater SD, suggesting that there could be a high conversion of IAA to oxIAA in these cell types or that the oxIAA formed is rapidly metabolized and/or transported out of the cells. The ratio between GFP+ and GFP− cells for IAA (Figure 7C) was highest in the M0028:GFP line, in accordance with previous data (Petersson et al., 2009).

OxIAA Is Not Active in Auxin-Specific Transport Across the Plasma Membrane and in Reporter Assays

Suspension-grown tobacco (*Nicotiana tabacum*) Bright Yellow (BY)-2 cells represent a useful tool for kinetic studies of the transport of auxin and auxin-related compounds (Petrášek et al., 2006). In most tobacco cell lines, the auxin influx and efflux carriers differ in terms of specificity toward synthetic auxins, 2,4-D being a good substrate for auxin influx machinery but a weak substrate for the efflux machinery. Conversely, naphthalene-1-acetic acid (NAA) is a good substrate for active efflux but a weak substrate for active influx (Delbarre et al. 1996). As such, the influx and efflux steps of the active auxin transport can be followed separately by accumulation assays, where a simple displacement of [^{3}H]2,4-D and [^{3}H]NAA with experimental compounds reflects the auxin influx and efflux activities, respectively. We used this auxin accumulation assay to analyze whether oxIAA is transported across plasma membranes, utilizing the auxin transport machinery for cell-to-cell transport. We did not observe displacement of [^{3}H]2,4-D or [^{3}H]NAA with 10 μM oxIAA, indicating that oxIAA does not interfere with the auxin transport machinery (Figure 8).

To assess the auxinic nature of oxIAA, we measured its ability to induce activity of the synthetic auxin response promoter DR5 in roots of *DR5rev*:*GFP*-expressing *Arabidopsis* seedlings (Benková et al., 2003). In control seedlings, the GFP signal was observed in the quiescent center, columella initials, and columella (Figures 9A and 9D; see Supplemental Figures 1A and 1B online). No increase in the GFP signal was observed in seedlings treated with 1 μM oxIAA for 4 h (Figure 9C; see Supplemental Figure 1C online), while the GFP signal was strongly increased in seedlings treated with 1 μM IAA under the same conditions (Figure 9B; see Supplemental Figure 1C online).

We then increased the concentration of IAA and oxIAA to 5, 10, and 100 μM and the duration of the treatment up to 24 h. Roots treated for 4 h with high concentrations of IAA showed a very strong GFP signal in the root tip (Figure 9B; see Supplemental Figures 1A and 1C online). The effect was even more pronounced after 24 h of IAA treatment, where changes in root morphology also started to appear (Figure 9E; see Supplemental Figures 1B and 1D online). Compared with IAA, oxIAA induced a very weak GFP response after 4 h of treatment

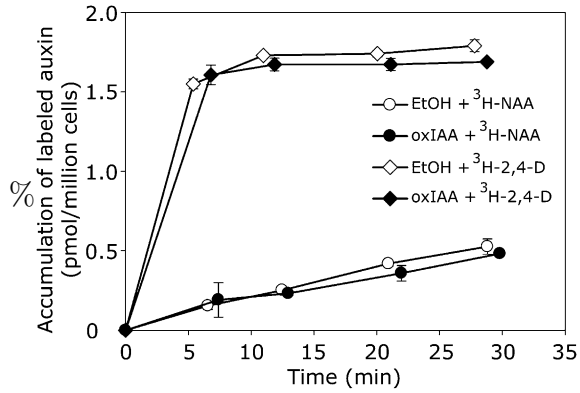

Figure 8. Activity of OxIAA in Auxin Transport Assays.

Competition of oxIAA (10 μM) with the accumulation of [^{3}H]2,4-D or [^{3}H]NAA, as markers of active auxin influx and efflux, respectively, is shown using suspension-cultured tobacco BY-2 cells. OxIAA did not compete with labeled 2,4-D or NAA for carrier-driven transport across the plasma membrane. Ethanol (EtOH) was used as a control. Error bars indicate SD (n = 4).

with 10 and 100 μM oxIAA, while no increase in the GFP signal was observed after the 24-h treatments (see Supplemental Figure 1 online).

Taken together, our data suggest that the catabolite oxIAA does not elicit an auxin-like response in the *Arabidopsis* root, nor is it subject to auxin-specific transport across the plasma membrane.

OxIAA Is Much Less Active Than IAA in Growth Assays and in Pull-Down Assays

To further explore the activity of oxIAA in vivo, we examined the effect of the compound on root and hypocotyl elongation in *Arabidopsis* seedlings. Hypocotyl elongation was induced by 0.5 to 50 μM IAA but was completely unaffected by oxIAA, even at high concentrations (up to 1000 μM; see Supplemental Figure 2 online). By comparison, IAA was very effective at inhibiting root elongation, with an almost complete inhibition at a concentration of 1 μM (Figure 10). At this concentration, oxIAA had no effect on root elongation, and only at very high oxIAA concentrations (>10 μM) could an effect on root growth be observed.

We also performed pull-down assays using TIR1-Myc and different GLUTATHIONE *S*-TRANSFERASE (GST)-IAA proteins expressed in vitro to determine if oxIAA interacted with the TIR1 auxin receptor. TIR1 was detected with the anti-c-Myc antibody. As expected, different concentrations of IAA enhanced the recovery of TIR1-Myc in the pull-down assays using GST-IAA3 and GST-IAA6 as input (Figures 11A and 11B). In contrast, comparable concentrations of oxIAA had no effect on the recovery of TIR1-Myc, indicating that the compound does not bind to the TIR1-IAA3 or TIR1-IAA6 coreceptor complex with high affinity. Surprisingly, both IAA and oxIAA increased the recovery of TIR1-Myc in TIR1-IAA7 pull-down assays, suggesting a strong binding of IAA and oxIAA to GST-IAA7 (Figure 11C). For GST-IAA7,

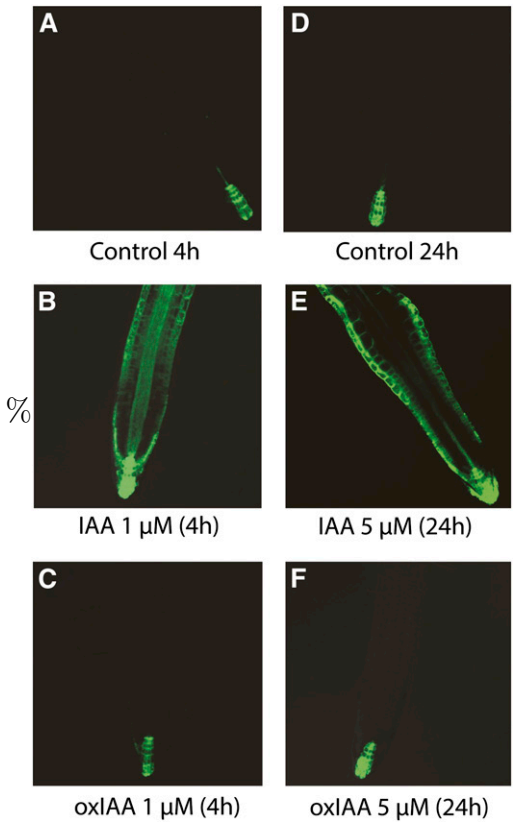

Figure 9. *DR5rev*:*GFP* Expression after IAA and OxIAA Treatment.

The expression of the *DR5rev*:*GFP* auxin-inducible reporter was examined after 4 h (**[A]** to **[C]**) and 24 h (**[D]** to **[F]**) of IAA and oxIAA treatment. No difference was observed between roots treated with 5 μM oxIAA for 24 h **(F)** and control roots **(D)**.
[See online article for color version of this figure.]

higher nonspecific binding was also observed (Figure 11C, mock treatment). It was previously shown that IAA7 interacts with TIR1 in the absence of IAA (Calderón Villalobos et al., 2012).

DISCUSSION

The establishment and maintenance of auxin gradients and auxin maxima and minima are integral to the regulation of auxin activity. Homeostasis of the hormone through conjugation and catabolism has been proposed to be a significant contributor to these processes. However, our limited knowledge of how these processes are regulated has made it difficult to explore their importance in maintaining appropriate hormone levels in specific tissues and cell types.

In this article, we have shown that the formation of oxIAA through a nondecarboxylative metabolism (i.e., with retention of the carboxylic group in the side chain) is a major pathway for IAA degradation in *Arabidopsis*. OxIAA was the major primary IAA metabolite detected in wild-type *Arabidopsis* roots, while IAA conjugates such as IAA-Asp and IAA-Glu were observed in much lower concentrations (Figure 2). OxIAA was highly abundant in the IAA-overproducing mutant lines *sur1-3* and *sur2-1* (Figure 2A), and the catabolite was rapidly formed after feeding *Arabidopsis* wild-type seedlings with exogenous IAA (Figures 5 and 6) and IAA precursors (Figure 3). Together, these findings indicated that oxIAA formation was an important pathway for IAA degradation in the *Arabidopsis* root and one of the major mechanisms for the regulation of IAA homeostasis in plants with constitutive IAA overproduction.

The auxin response reporter *DR5rev*:*GFP* was rapidly induced by IAA treatment but had a very low response to oxIAA, even under long exposures and high concentrations of the hormone (Figure 9; see Supplemental Figure 1 online). In the root elongation assay, more than 1000 times higher concentration of oxIAA than IAA was needed to observe any morphological effect (Figure 10). This indicated that oxIAA is a true catabolite that is not biologically active and is not converted back to active IAA under physiological conditions. The very weak effect that we could observe in these assays may indicate that high concentrations of exogenous oxIAA have a nonspecific effect. However, it cannot be ruled out that the compound has a weak IAA-like activity at nonbiologically relevant concentrations or that exogenous oxIAA is slowly converted to IAA. It is also possible that oxIAA perturbs endogenous IAA metabolism when fed at high concentrations. In order to further determine the potential for activity of the compound, we compared oxIAA activity with the activity of the natural auxin IAA. The TIR1/AFB proteins are the major IAA receptors for transcriptional auxin signaling (Calderon-Villalobos et al., 2010). In pull-down assays, oxIAA did not bind to the TIR1-IAA3 and TIR1-IAA6 coreceptor complexes (Figures 11A and 11B). As the difference between the IAA and the oxIAA molecules lies in the indole ring, and the extra oxygen changes the hydrophobicity and the size of the indole structure, this most likely leads to a decrease in the binding affinity of the compound to the receptor (Calderon-Villalobos et al., 2010). In contrast to our results with IAA3 and IAA6, oxIAA strongly promoted the interaction of IAA7 with TIR1

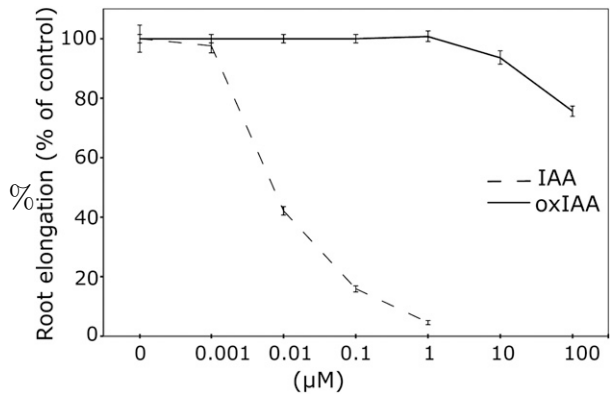

Figure 10. Activity of IAA and OxIAA in Root Elongation Assays.

Root elongation was measured after treating 5-DAG wild-type *Arabidopsis* Col-0 seedlings with different concentrations of IAA and oxIAA for 3 d. IAA effectively inhibits root elongation in concentrations below 1 μM. At these concentrations, oxIAA has no effect on cell elongation in the root. Error bars indicate SE (n = 12).

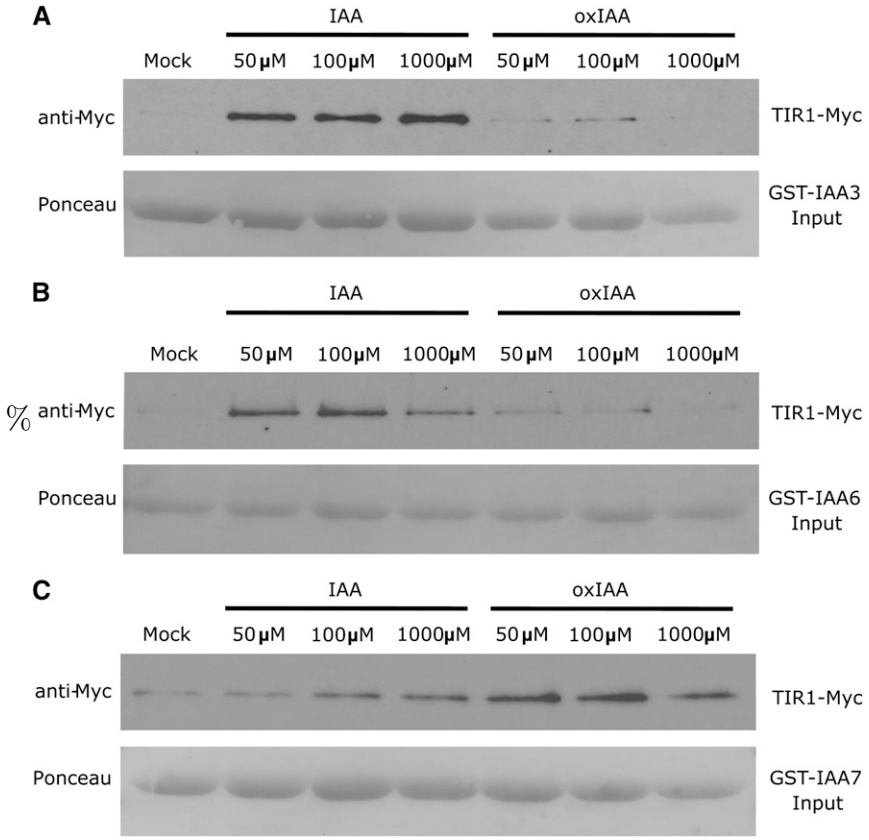

Figure 11. Binding of IAA and OxIAA to TIR1/IAAs in Pull-Down Assays.

Pull-down experiments were performed using in vitro–translated TIR1-Myc and recombinant GST-IAA3 **(A)**, GST-IAA6 **(B)**, and GST-IAA7 **(C)** proteins. Ponceau S dye was used for protein detection. Reactions were incubated for 60 min in the presence or absence of 50, 100, or 1000 μM IAA or oxIAA.

(Figure 11C). At this point, the basis for this difference is unknown. However, we note that IAA7 shows more nonspecific binding than the other proteins and can interact with TIR1 in the absence of IAA (Calderón Villalobos et al., 2012). Our data open up the possibility that oxIAA could bind to the auxin receptor under specific conditions or in specific cell types, depending on the expression levels of the different Aux/IAA proteins. Further studies will be required to test this idea.

Our data also showed that oxIAA did not interfere with the accumulation in cells of 2,4-D and NAA, which are known to be good substrates for the plasma membrane–located auxin carriers (Delbarre et al., 1996; Petrášek et al., 2006; Simon et al., 2013). This indicates that oxIAA is not transported via the auxin influx or efflux carriers (Figure 8). It has recently been suggested that oxIAA could instead function as a substrate for the ABC SUBFAMILY G (ABCG) transporters ABCG36/ABCG37. ABCG transporters are known to transport a large variety of organic molecules (reviewed in Verrier et al., 2008), and the proposed function in *Arabidopsis* roots would be to transport oxIAA out of the root epidermis (Peer et al., 2013).

By analyzing IAA and the major IAA catabolites and conjugates in the *Arabidopsis* root apex, we observed that the oxIAA concentration closely followed the IAA gradient, with high IAA and oxIAA concentrations in the most apical sections of the primary root (Figure 4). The concentrations of the other major IAA conjugates (IAA-Asp and IAA-Glu) were much lower and did not resemble the IAA gradient. This is a further indication that oxIAA is one of the major primary degradation products of IAA in the root apex. To date, very little has been known about the role of IAA degradation in the homeostatic regulation of IAA levels in the root. The root apex can be considered both as an IAA sink (mainly originating from shoot tissues; reviewed in Robert and Friml, 2009) and as a source of IAA (synthesized in the root tip itself; Ljung et al., 2005; Petersson et al., 2009). Although growth of the root has the potential to result in the continual dilution of the auxin concentration within the root apex, and some auxin is actively transported away from the tip, it is likely that IAA conjugation and degradation processes are important for maintaining the auxin gradient and avoiding overaccumulation of the hormone in the root tip. To date, only genes involved in IAA conjugation have been identified in plants (reviewed in Normanly, 2010; Ludwig-Müller, 2011; Korasick et al., 2013; Ljung, 2013). To be able to answer whether general, constitutive catabolic activity is present in most cells of the root apex, or if specific catabolic sites exist in certain cell types, we performed cell type–specific analysis of IAA and oxIAA levels in four different

Arabidopsis lines expressing GFP in specific cell types of the root apex (Figure 7). Our data indicate that there are differences in catabolic activity between root cell types, suggesting that cells with strong activity are specifically involved in auxin gradient formation and maintenance in the root. The finding that the levels of both IAA and oxIAA were highest in the root cap, the columella, the columella initials, and the quiescent center suggests that these cell types act as active sites for the removal of auxin from the root-ward auxin stream.

Taken together, our data strongly indicate that oxIAA is an irreversible IAA catabolite with very low, if any, auxin activity. In order to determine the precise mechanism of oxIAA formation and its role in IAA gradient formation during plant development, it will be important to identify the genes involved in these metabolic pathways and to understand how they are regulated. The work described here provides the necessary empirical evidence that IAA conversion to oxIAA plays an important role in regulating auxin levels and paves the way for a more detailed analysis of the regulation of the process and its consequences for plant function.

METHODS

Plant Material and Growth Conditions

Seeds of wild-type *Arabidopsis thaliana* Col-0 and the mutant lines *35S*:*YUC1*, *sur2-1*, and *sur1-3* were surface-sterilized and plated on solid Murashige and Skoog (MS) medium (1× MS medium [Duchefa], 1% Suc, and 1% agar [Merck], pH 5.7). The GFP lines used in this study, *pWOL*:*GFP*, *pSCR*:*GFP*, J2812:GFP, and M0028:GFP, have been described (Petersson et al., 2009). For the collection of larger amounts of root material for protoplasting and cell sorting, seeds were sown at high density (~500 seeds per row) on a nylon mesh (Sefar Nitex, 03-110/47) placed on solid MS medium. After vernalization at 4°C for 3 to 4 d, the plates were placed vertically under 150 μE light in LD conditions (16 h of light, 8 h of darkness) at 22°C.

Quantification of IAA Metabolites

For the quantification of IAA metabolites, *Arabidopsis* Col-0 and mutant lines were grown in LD conditions for 10 d. Homozygous seedlings of the *sur1-3* mutant line were selected from the plates. Seedlings were divided into shoot and root, and 20 mg of root tissue per sample was collected in triplicate. For the quantification of IAA metabolites in the root apex, 1-mm sections of the primary root apex of 6-d-old *Arabidopsis* Col-0 seedlings were collected in triplicate (200 1-mm sections were pooled for each biological replicate).

Frozen samples were homogenized using a MixerMill MM 301 bead mill (Retsch) at a frequency of 25 Hz for 5 min after adding 3-mm tungsten carbide beads (Qiagen; catalog No. 69,997) and extracted in 1 mL of 50 mM sodium phosphate buffer (pH 7.0) containing 0.02% sodium diethyldithiocarbamate and the following $^{13}C_6$-labeled internal standards: [indole-$^{13}C_6$]IAA, [indole-$^{13}C_6$]oxIAA, [indole-$^{13}C_6$]IAA-Asp, and [indole-$^{13}C_6$]IAA-Glu. The samples were incubated at 4°C with continuous shaking and then centrifuged (15 min, 23,000*g* at 4°C). The pH was adjusted to 2.7 with 1 M hydrochloric acid, and the samples were purified by solid-phase extraction (SPE). First, the root apex extracts were purified on 30-mg Oasis MAX columns (Waters). After sample application, the columns were washed with 1 mL of 5 mM ammonium hydroxide and eluted with 1.5 mL of acetonitrile containing 2% (v/v) formic acid. The eluates were vacuum-dried, dissolved in 25 μL of methanol, and reacted with 225 μL of diazomethane in diethylether for 30 min. Excess derivatization reagent was quenched with 100 μL of 2 M acetic acid in *n*-heptane, and the samples were dried in a stream of nitrogen. Samples were then reconstituted with 10 μL of 10% acetonitrile prior to analysis by LC-MS/MS, as described by Kowalczyk and Sandberg (2001). Second, the wild-type and mutant root samples were purified on Oasis hydrophilic-lipophilic balance reversed-phase sorbent columns (30 mg; Waters) conditioned with 1 mL of methanol, 1 mL of water, and 0.5 mL of sodium phosphate buffer (pH 2.7). After sample application, the column was washed with 2 mL of 5% methanol and then eluted with 2 mL of 80% methanol. Eluates were evaporated to dryness and dissolved in 20 μL of mobile phase prior to mass analysis using a 1290 Infinity LC system and 6460 Triple Quadrupole LC/MS system (Agilent Technologies; Novák et al., 2012).

Profiling of IAA Metabolites after Feeding with Labeled and Unlabeled IAA and IAA Precursors

Seven-day-old *Arabidopsis* Col-0 seedlings were incubated with liquid medium containing 10 μM [$^{15}N_1$]anthranilate or [$^{15}N_1$]indole for 3, 6, 12, and 24 h under gentle shaking and in darkness. For each replicate, 20 mg of seedlings was extracted and purified by SPE on hydrophilic-lipophilic balance reversed-phase sorbent columns as described above for IAA metabolites. The incorporation of the label into IAA and oxIAA was measured using LC-MS/MS, with the multiple reaction monitoring transitions *m/z* 176.1 > *m/z* 130.1 and *m/z* 192.1 > *m/z* 146.1 for endogenous and *m/z* 177.1 > *m/z* 131.1 and *m/z* 193.1 > *m/z* 147.1 for labeled IAA and oxIAA, respectively. De novo synthesis of IAA and oxIAA was calculated as the isotope ratio, that is, the ratio of labeled to unlabeled IAA (*m/z* 131.1:130.1) and oxIAA (*m/z* 147.1:146.1) after correction for natural isotope abundances (Cobelli et al., 1992).

Seven-day-old *Arabidopsis* Col-0 seedlings (five to seven seedlings, 0.7–1.2 g fresh weight) were incubated with 0.75 mL of sterile MS medium containing 1 μM [1′-^{14}C]IAA (American Radiolabeled Chemicals) for 8 h. For incubations of roots, the aerial parts of the seedlings were removed with a scalpel, and ~1 μg (0.3 μCi) of [1′-^{14}C]IAA dissolved in 0.5 mL of sterile 0.3% agar was applied just above the cutting line. After 8 h, root tips (around 5 mm) were collected and washed with distilled water, and protoplasts were isolated as described by Petersson et al. (2009). Samples of intact root tips and whole seedlings were also prepared. Whole seedlings and intact root tips were homogenized as described previously in 1 mL of ice-cold 50 mM sodium phosphate buffer, pH 7. Protoplast samples were sonicated for 3 min in the protoplast preparation buffer using a T460 sonicator (Elma Gmbh & Co KG). Samples were then acidified and purified using 50-mg C18 Bond Elut SPE columns as described by Petersson et al. (2009). After purification, samples were evaporated and dissolved in 100 μL of 10% methanol. An aliquot of each sample, containing ~0.05 μCi, was injected, and HPLC analysis combined with radioactive scintillation counting was performed as described by Östin et al. (1998). For samples containing low amounts of radioactivity, 1-min fractions were collected, and their radioactivity was measured using a Beckman LS6500 scintillation counter.

Eight-day-old *Arabidopsis* Col-0 seedlings were also incubated for 5.5 h in liquid medium with and without 10 μM IAA. Root apices (5 mm) were collected and pooled for quantification of oxIAA using LC-MS/MS as described previously. Each sample consisted of 10 root apices, and the samples were analyzed in five replicates.

Cell Type–Specific Analysis of IAA and OxIAA Levels

The *Arabidopsis* lines *pWOL*:*GFP*, *pSCR*:*GFP*, J2812:GFP, and M0028:GFP were grown on vertical plates in long days for 8 d as described. Root tissues were collected and treated with cell wall–degrading enzymes, and protoplasts were isolated and sorted by FACS as described by Petersson

et al. (2009) and Jones et al. (2010) with minor modifications. A total of 200,000 protoplasts were collected for each biological and technical replicate (for both the GFP+ and GFP− cell populations), except for the M0028:GFP line, where 20,000 to 100,000 protoplasts were collected for each replicate. Amounts of 5 pmol of [$^{13}C_6$]IAA and 1 pmol of [$^{13}C_6$]oxIAA were added as internal standards, and the samples were frozen to rupture the plasma membrane. Samples were purified by in-tip solid-phase microextraction using a modification of the protocol described by Svačinová et al. (2012). After application of the sample, the microcolumn was washed with 1% acetic acid, and IAA and oxIAA were eluted using methanol. Quantification of IAA and oxIAA was performed by LC-MS/MS according to Novák et al. (2012). The numbers of biological replicates analyzed were as follows: *pWOL*:*GFP* (8), *pSCR*:*GFP* (9), J2812:GFP (11), and M0028:GFP (7). For each biological GFP+ replicate, GFP− cells were collected and used as reference samples, analyzed in two technical replicates.

Cultivation of BY-2 Tobacco Cells and Auxin Accumulation Assays

Cells of the tobacco (*Nicotiana tabacum*) line BY-2 (Nagata et al., 1992) were cultivated in liquid cultivation medium (3% Suc, 4.3 g L^{-1} MS salts, 100 mg L^{-1} inositol, 1 mg L^{-1} thiamine, 0.2 mg L^{-1} 2,4-D, and 200 mg L^{-1} KH_2PO_4, pH 5.8) at 25°C in darkness on an orbital incubator (120 rpm, orbital diameter of 3 cm; IKA KS501, IKA Labortechnik [http://www.ika.net]) and subcultured weekly. Stock calli were maintained on the same medium, solidified with 0.6% (w/v) agar.

Auxin accumulation was determined in BY-2 tobacco cells using the protocol described were provided by American Radiolabeled Chemicals (http://www.arcincusa.com) at the molar radioactivity of 20 Ci $mmol^{-1}$. The accumulation in cells was measured in 0.5-mL aliquots of cell suspension (cell density of $\sim 7 \times 10^5$ cells mL^{-1}, as determined by counting cells in a Fuchs–Rosenthal hemocytometer). OxIAA (10 μM) was added to the cell suspension immediately after the application of radiolabeled auxin (2 nM).

DR5rev:*GFP* Induction Assays

Four-day-old *Arabidopsis DR5rev*:*GFP* seedlings (Benková et al., 2003) were transferred to sterile liquid medium (2.3 g L^{-1} MS salts, 0.5 g L^{-1} MES [pH 5.8], 1% [w/v] Suc, and 0.1 g L^{-1} *myo*-inositol). OxIAA and IAA were applied in a particular concentration (1, 5, 10, or 100 μM), and the seedlings were incubated for 4 or 24 h on an orbital shaker (150 rpm) under a yellow filter (Stasinopoulos and Hangarter, 1990). The GFP signal was observed using an LSM510 confocal laser scanning microscope (Carl Zeiss) with an excitation of 488 nm using an argon laser and a 20× objective. The GFP fluorescence intensity of the meristematic zone was measured using the image-analysis software ImageJ (http://rsb.info.nih.gov/ij/) from 15 primary root tips per treatment.

Root and Hypocotyl Elongation Assays

To determine the effects of auxin on root elongation, 5-d-old *Arabidopsis* Col-0 seedlings grown in LD conditions were transferred to plates with various concentrations of IAA or oxIAA for 3 d, after which the root length after transfer was measured using ImageJ software (http://rsbweb.nih.gov/ij/index.html). Growth was expressed as a percentage of growth on medium without exogenous IAA or oxIAA. For each treatment, 12 seedlings were analyzed. To determine the effects of auxin on hypocotyl elongation, 5-d-old *Arabidopsis* Col-0 seedlings were transferred onto plates with various concentrations of IAA or oxIAA for 48 h. Hypocotyl images were captured with a Nikon dissecting microscope, and the hypocotyl length was measured with ImageJ software. For each treatment, 24 seedlings were analyzed. Seedlings were germinated and treated under a LD light cycle.

Protein Expression and Pull-Down Experiments

The pull-down assay was performed as described by Yu et al. (2013). TIR1-Myc was produced from the TNT T7 coupled wheat germ extract system (Promega; catalog No. L4140), and GST-IAA proteins were expressed in the *Escherichia coli* BL21DE3 strain and purified with Glutathione-Agarose (Sigma-Aldrich; catalog No. G4510). Twenty microliters of TIR1-Myc and 50 μL of GST-IAA3 or GST-IAA6 were incubated in 300 μL of pull-down buffer in the presence or absence of 50, 100, and 1000 μM IAA or oxIAA for 60 min. For the pull-down assay with IAA7, 10 μL of GST-IAA7 was added as input. The eluted products were detected by anti-c-Myc-peroxidase antibody (Roche; catalog No. 11814150001) at a dilution of 1:10,000. Ponceau S (Sigma; catalog No. P3504) was used for protein detection at a concentration of 0.1% Ponceau S (w/v) in 5% acetic acid solution.

Accession Numbers

The origins of the knockout and overexpressing lines analyzed in this article are as follows: YUCCA1-35S:YUC1, At4g32540; CYP83B1-sur2-1, At4g31500; and C-S lyase-sur1-3, At2g20610.

Supplemental Data

The following materials are available in the online version of this article.

Supplemental Figure 1. *DR5rev*:*GFP* Expression after IAA and oxIAA Treatment.

Supplemental Figure 2. Activity of IAA and oxIAA in Hypocotyl Elongation Assays.

ACKNOWLEDGMENTS

The *Arabidopsis* mutant lines used in this study were generous gifts from Catherine Bellini and Yunde Zhao, and the *DR5rev*:*GFP* seeds were kindly provided by Eva Benková. The GFP lines were obtained from Philip Benfey (*pWOL*:*GFP* and *pSCR*:*GFP*) and from the Nottingham Arabidopsis Stock Centre (J2812:GFP and M0028:GFP). We also thank Roger Granbom and Gun Lövdahl for excellent technical assistance. This work was supported by the Swedish Governmental Agency for Innovation Systems, the Swedish Research Council, and the Marianne and Marcus Wallenberg Foundation (to K.L., O.N., and G.S.), the Kempe Foundation (to A.P. and B.S.), the Internal Grant Agency of Palacký University (PrF_2013_023; to O.N. and E.H.), the U.S. National Institutes of Health (to M.E,.), and the Grant Agency of the Czech Republic (project P305/11/0797; to E.Z.).

AUTHOR CONTRIBUTIONS

K.L. and G.S. conceived the study and wrote the article with substantial input from S.V.P., A.P., and O.N. A.P, S.V.P., G.S., and K.L. designed the research. A.P., B.S., S.V.P., E.H., S.S., K.G., Y.Z., M.K., and O.N. performed the research, and M.E. and E.Z. analyzed the data. A.P., O.N., and M.K. contributed new analytical tools. All authors read and approved the final article for publication.

Received June 4, 2013; revised October 2, 2013; accepted October 9, 2013; published October 25, 2013.

REFERENCES

Barbez, E., et al. (2012). A novel putative auxin carrier family regulates intracellular auxin homeostasis in plants. Nature **485:** 119–122.

Barlier, I., Kowalczyk, M., Marchant, A., Ljung, K., Bhalerao, R., Bennett, M., Sandberg, G., and Bellini, C. (2000). The *SUR2* gene of *Arabidopsis thaliana* encodes the cytochrome P450 CYP83B1, a modulator of auxin homeostasis. Proc. Natl. Acad. Sci. USA **97:** 14819–14824.

Benková, E., Ivanchenko, M.G., Friml, J., Shishkova, S., and Dubrovsky, J.G. (2009). A morphogenetic trigger: Is there an emerging concept in plant developmental biology? Trends Plant Sci. **14:** 189–193.

Benková, E., Michniewicz, M., Sauer, M., Teichmann, T., Seifertová, D., Jürgens, G., and Friml, J. (2003). Local, efflux-dependent auxin gradients as a common module for plant organ formation. Cell **115:** 591–602.

Bhalerao, R.P., and Bennett, M.J. (2003). The case for morphogens in plants. Nat. Cell Biol. **5:** 939–943.

Boerjan, W., Cervera, M.T., Delarue, M., Beeckman, T., Dewitte, W., Bellini, C., Caboche, M., Van Onckelen, H., Van Montagu, M., and Inzé, D. (1995). Superroot, a recessive mutation in *Arabidopsis*, confers auxin overproduction. Plant Cell **7:** 1405–1419.

Calderon-Villalobos, L.I., Tan, X., Zheng, N., and Estelle, M. (2010). Auxin perception—Structural insights. Cold Spring Harb. Perspect. Biol. **2:** a005546.

Calderón Villalobos, L.I.A., et al. (2012). A combinatorial TIR1/AFB-Aux/IAA co-receptor system for differential sensing of auxin. Nat. Chem. Biol. **8:** 477–485.

Cobelli, C., Toffolo, G., and Foster, D.M. (1992). Tracer-to-tracee ratio for analysis of stable isotope tracer data: Link with radioactive kinetic formalism. Am. J. Physiol. **262:** E968–E975.

Dal Bosco, C., et al. (2012). The endoplasmic reticulum localized PIN8 is a pollen-specific auxin carrier involved in intracellular auxin homeostasis. Plant J. **71:** 860–870.

Delbarre, A., Muller, P., Imhoff, V., and Guern, J. (1996). Comparison of mechanisms controlling uptake and accumulation of 2,4-dichlorophenoxy acetic acid, naphthalene-1-acetic acid, and indole-3-acetic acid in suspension-cultured tobacco cells. Planta **198:** 532–541.

Dharmasiri, N., Dharmasiri, S., and Estelle, M. (2005). The F-box protein TIR1 is an auxin receptor. Nature **435:** 441–445.

Ding, Z., et al. (2012). ER-localized auxin transporter PIN8 regulates auxin homeostasis and male gametophyte development in Arabidopsis. Nat Commun **3:** 941.

Ernstsen, A., Sandberg, G., and Lundström, K. (1987). Identification of oxindole-3-acetic acid, and metabolic conversion of indole-3-acetic acid to oxindole-3-acetic acid in seeds of *Pinus sylvestris*. Planta **172:** 47–52.

Gallavotti, A., Barazesh, S., Malcomber, S., Hall, D., Jackson, D., Schmidt, R.J., and McSteen, P. (2008). sparse inflorescence1 encodes a monocot-specific YUCCA-like gene required for vegetative and reproductive development in maize. Proc. Natl. Acad. Sci. USA **105:** 15196–15201.

Jones, B., Gunnerås, S.A., Petersson, S.V., Tarkowski, P., Graham, N., May, S., Dolezal, K., Sandberg, G., and Ljung, K. (2010). Cytokinin regulation of auxin synthesis in *Arabidopsis* involves a homeostatic feedback loop regulated via auxin and cytokinin signal transduction. Plant Cell **22:** 2956–2969.

Kai, K., Horita, J., Wakasa, K., and Miyagawa, H. (2007). Three oxidative metabolites of indole-3-acetic acid from *Arabidopsis thaliana*. Phytochemistry **68:** 1651–1663.

Kepinski, S., and Leyser, O. (2005). The *Arabidopsis* F-box protein TIR1 is an auxin receptor. Nature **435:** 446–451.

Korasick, D.A., Enders, T.A., and Strader, L.C. (2013). Auxin biosynthesis and storage forms. J. Exp. Bot. **64:** 2541–2555.

Kowalczyk, M., and Sandberg, G. (2001). Quantitative analysis of indole-3-acetic acid metabolites in Arabidopsis. Plant Physiol. **127:** 1845–1853.

Kubeš, M., et al. (2012). The Arabidopsis concentration-dependent influx/efflux transporter ABCB4 regulates cellular auxin levels in the root epidermis. Plant J. **69:** 640–654.

Ljung, K. (2013). Auxin metabolism and homeostasis during plant development. Development **140:** 943–950.

Ljung, K., Hull, A.K., Celenza, J., Yamada, M., Estelle, M., Normanly, J., and Sandberg, G. (2005). Sites and regulation of auxin biosynthesis in *Arabidopsis* roots. Plant Cell **17:** 1090–1104.

Ludwig-Müller, J. (2011). Auxin conjugates: Their role for plant development and in the evolution of land plants. J. Exp. Bot. **62:** 1757–1773.

Mashiguchi, K., et al. (2011). The main auxin biosynthesis pathway in Arabidopsis. Proc. Natl. Acad. Sci. USA **108:** 18512–18517.

Mikkelsen, M.D., Naur, P., and Halkier, B.A. (2004). *Arabidopsis* mutants in the C-S lyase of glucosinolate biosynthesis establish a critical role for indole-3-acetaldoxime in auxin homeostasis. Plant J. **37:** 770–777.

Mravec, J., et al. (2009). Subcellular homeostasis of phytohormone auxin is mediated by the ER-localized PIN5 transporter. Nature **459:** 1136–1140.

Nagata, T., Nemoto, Y., and Hasezawa, S. (1992). Tobacco BY-2 cell line as the "HeLa" cell in the cell biology of higher plants. Int. Rev. Cytol. **132:** 1–30.

Normanly, J. (2010). Approaching cellular and molecular resolution of auxin biosynthesis and metabolism. Cold Spring Harb. Perspect. Biol. **2:** a001594.

Novák, O., Hényková, E., Sairanen, I., Kowalczyk, M., Pospíšil, T., and Ljung, K. (2012). Tissue-specific profiling of the *Arabidopsis thaliana* auxin metabolome. Plant J. **72:** 523–536.

Östin, A., Kowalyczk, M., Bhalerao, R.P., and Sandberg, G. (1998). Metabolism of indole-3-acetic acid in Arabidopsis. Plant Physiol. **118:** 285–296.

Peer, W.A., Cheng, Y., and Murphy, A.S. (2013). Evidence of oxidative attenuation of auxin signalling. J. Exp. Bot. **64:** 2629–2639.

Petersson, S.V., Johansson, A.I., Kowalczyk, M., Makoveychuk, A., Wang, J.Y., Moritz, T., Grebe, M., Benfey, P.N., Sandberg, G., and Ljung, K. (2009). An auxin gradient and maximum in the *Arabidopsis* root apex shown by high-resolution cell-specific analysis of IAA distribution and synthesis. Plant Cell **21:** 1659–1668.

Petrášek, J., et al. (2006). PIN proteins perform a rate-limiting function in cellular auxin efflux. Science **312:** 914–918.

Quittenden, L.J., Davies, N.W., Smith, J.A., Molesworth, P.P., Tivendale, N.D., and Ross, J.J. (2009). Auxin biosynthesis in pea: Characterization of the tryptamine pathway. Plant Physiol. **151:** 1130–1138.

Rampey, R.A., LeClere, S., Kowalczyk, M., Ljung, K., Sandberg, G., and Bartel, B. (2004). A family of auxin-conjugate hydrolases that contributes to free indole-3-acetic acid levels during Arabidopsis germination. Plant Physiol. **135:** 978–988.

Reinecke, D.M., and Bandurski, R.S. (1983). Oxindole-3-acetic acid, an indole-3-acetic acid catabolite in *Zea mays*. Plant Physiol. **71:** 211–213.

Robert, H.S., and Friml, J. (2009). Auxin and other signals on the move in plants. Nat. Chem. Biol. **5:** 325–332.

Sauer, M., Robert, S., and Kleine-Vehn, J. (2013). Auxin: Simply complicated. J. Exp. Bot. **64:** 2565–2577.

Simon, S., Kubeš, M., Baster, P., Robert, S., Dobrev, P.I., Friml, J., Petrášek, J., and Zažímalová, E. (August 5, 2013). Defining the selectivity of processes along the auxin response chain: A study using auxin analogues. New Phytol. http://dx.doi.org/10.1111/nph.12437.

Stasinopoulos, T.C., and Hangarter, R.P. (1990). Preventing photochemistry in culture media by long-pass light filters alters growth of cultured tissues. Plant Physiol. **93:** 1365–1369.

Staswick, P.E. (2009). The tryptophan conjugates of jasmonic and indole-3-acetic acids are endogenous auxin inhibitors. Plant Physiol. **150:** 1310–1321.

Stepanova, A.N., Robertson-Hoyt, J., Yun, J., Benavente, L.M., Xie, D.Y., Dolezal, K., Schlereth, A., Jürgens, G., and Alonso, J.M.

(2008). TAA1-mediated auxin biosynthesis is essential for hormone crosstalk and plant development. Cell **133:** 177–191.

Stepanova, A.N., Yun, J., Robles, L.M., Novák, O., He, W., Guo, H., Ljung, K., and Alonso, J.M. (2011). The *Arabidopsis* YUCCA1 flavin monooxygenase functions in the indole-3-pyruvic acid branch of auxin biosynthesis. Plant Cell **23:** 3961–3973.

Sugawara, S., Hishiyama, S., Jikumaru, Y., Hanada, A., Nishimura, T., Koshiba, T., Zhao, Y., Kamiya, Y., and Kasahara, H. (2009). Biochemical analyses of indole-3-acetaldoxime-dependent auxin biosynthesis in Arabidopsis. Proc. Natl. Acad. Sci. USA **106:** 5430–5435.

Svačinová, J., Novák, O., Plačková, L., Lenobel, R., Holík, J., Strnad, M., and Doležal, K. (2012). A new approach for cytokinin isolation from Arabidopsis tissues using miniaturized purification: Pipette tip solid-phase extraction. Plant Methods **8:** 17.

Tam, Y.Y., Epstein, E., and Normanly, J. (2000). Characterization of auxin conjugates in Arabidopsis. Low steady-state levels of indole-3-acetyl-aspartate, indole-3-acetyl-glutamate, and indole-3-acetyl-glucose. Plant Physiol. **123:** 589–596.

Tao, Y., et al. (2008). Rapid synthesis of auxin via a new tryptophan-dependent pathway is required for shade avoidance in plants. Cell **133:** 164–176.

Verrier, P.J., et al. (2008). Plant ABC proteins—A unified nomenclature and updated inventory. Trends Plant Sci. **13:** 151–159.

Won, C., Shen, X., Mashiguchi, K., Zheng, Z., Dai, X., Cheng, Y., Kasahara, H., Kamiya, Y., Chory, J., and Zhao, Y. (2011). Conversion of tryptophan to indole-3-acetic acid by TRYPTOPHAN AMINOTRANSFERASES OF ARABIDOPSIS and YUCCAs in Arabidopsis. Proc. Natl. Acad. Sci. USA **108:** 18518–18523.

Yamada, M., Greenham, K., Prigge, M.J., Jensen, P.J., and Estelle, M. (2009). The TRANSPORT INHIBITOR RESPONSE2 gene is required for auxin synthesis and diverse aspects of plant development. Plant Physiol. **151:** 168–179.

Yamamoto, Y., Kamiya, N., Morinaka, Y., Matsuoka, M., and Sazuka, T. (2007). Auxin biosynthesis by the YUCCA genes in rice. Plant Physiol. **143:** 1362–1371.

Yu, H., Moss, B.L., Jang, S.S., Prigge, M., Klavins, E., Nemhauser, J.L., and Estelle, M. (2013). Mutations in the TIR1 auxin receptor that increase affinity for auxin/indole-3-acetic acid proteins result in auxin hypersensitivity. Plant Physiol. **162:** 295–303.

Zažímalová, E., Murphy, A.S., Yang, H., Hoyerová, K., and Hošek, P. (2010). Auxin transporters–: Why so many? Cold Spring Harb. Perspect. Biol. **2**: a001552.

Zhao, Y., Christensen, S.K., Fankhauser, C., Cashman, J.R., Cohen, J.D., Weigel, D., and Chory, J. (2001). A role for flavin monooxygenase-like enzymes in auxin biosynthesis. Science **291:** 306–309.

Regulation of Auxin Homeostasis and Gradients in *Arabidopsis* Roots through the Formation of the Indole-3-Acetic Acid Catabolite 2-Oxindole-3-Acetic Acid

Ales Pencík, Biljana Simonovik, Sara V. Petersson, Eva Henyková, Sibu Simon, Kathleen Greenham, Yi Zhang, Mariusz Kowalczyk, Mark Estelle, Eva Za ζímalová, Ondrej Novák, Göran Sandberg and Karin Ljung

Plant Cell 2013;25;3858-3870; originally published online October 25, 2013;
DOI 10.1105/tpc.113.114421